The Interannual Variability of Climate in a Coupled Ocean–Atmosphere Model

Yu Yongqiang (俞永强) and *Guo Yufu* (郭裕福)
Institute of Atmospheric Physics, Chinese Academy of Sciences, Beijing 100029
Received November 14, 1994; revised December 8, 1994

ABSTRACT

In this paper, the interannual variability simulated by the coupled ocean–atmosphere general circulation model of the Institute of Atmospheric Physics (IAP CGCM) in 40 year integrations is analyzed, and compared with that by the corresponding IAP AGCM which uses the climatic sea surface temperature as the boundary condition in 25 year integrations.

The mean climatic states of January and July simulated by IAP CGCM are in good agreement with that by IAP AGCM, i.e., no serious 'climate drift' occurs in the CGCM simulation. A comparison of the results from AGCM and CGCM indicates that the standard deviation of the monthly averaged sea level pressure simulated by IAP CGCM is much greater than that by IAP AGCM in tropical region. In addition, both Southern Oscillation (SO) and North Atlantic Oscillation (NAO) can be found in the CGCM simulation for January, but these two oscillations do not exist in the AGCM simulation.

The interannual variability of climate may be classified into two types: one is the variation of the annual mean, another is the variation of the annual amplitude. The ocean–atmosphere interaction mainly increases the first type of variability. By means of the rotated EOF, the most important patterns corresponding to the two types of interannual variability are found to have different spatial and temporal characteristics.

Key words: Interannual variability of climate, Coupled ocean–atmosphere model

1. INTRODUCTION

The continuous drought, flood and severe winter have occurred frequently for dozens of years recently all over the world, which have caught people's concern with the climatic variability. Interannual variability of climate is an important aspect of studies on climate and climate change, and also one of the key projects of the World Climate Research Programme (WCRP). The interaction between atmosphere and the underlying surface (especially the ocean) plays a crucial role in the genesis of interannual variation of climate, but the cause of interannual variability is not well understood. The report of WCRP (WMO / ICSU,1984) pointed out that only on the basis of coupled ocean–atmosphere dynamics could the interannul variability be understood.

The coupled ocean–atmosphere general circulation model (CGCM) is a powerful tool which may simulate the interaction between the ocean and the atmosphere. Therefore CGCMs have been developed to simulate the coupled ocean–atmosphere system. The current CGCMs can reproduce the important features of contemporary climate, but great differences still exhibit in two essential aspects which are climate drift and interannual variability (Neelin et al, 1992). Most of the CGCMs suffer from climate drift, though some of them have used flux–correction method. Generally speaking, the interannual variability simulated by CGCMs is weaker than the observed.

Many studies have focused on analyzing the interannual variability of climate in general circulation models (GCMs). Manabe (1983) described some comparative results of temperature from 20-year-integration of a GCM coupled to an interactive ocean and indicated that the spectrum of the surface air temperature of the model with atmosphere-mixed layer ocean interaction over oceanic regions is much reder than the corresponding spectrum of the model without the air-sea interaction. Guo Yufu and Houghton (1991) analyzed results from a CGCM and found that SST anomalies around the Philippines have a close relation with the main precipitation variability pattern and the overall distribution of precipitation anomalies in Northern Hemisphere. In fact, the interannual variability has close relation with ENSO episodes and many people have paid great attention to the simulation of ENSO. ENSO events internally generated by a coupled model have been analyzed in detail (Meehl,1990). Chen (1992) also described the ENSO-alike phenomena simulated by the Institute of Atmospheric Physics (IAP)'s CGCM, and pointed out that IAP CGCM successfully simulates the westward propagation of SST from the coast of Peru.

The climate system which contains the atmosphere, hydrosphere, geosphere, icysphere and biosphere is a highly complex system. However the CGCM nowadays only includes the interaction between the atmosphere and the ocean. Although the CGCM is much simpler than the real climate system, the CGCM can help us to know the real climate system effectively. In this paper, a 25-year-integration of IAP's atmospheric general circulation model (AGCM) and 40-year-integration of IAP CGCM are analyzed. The monthly averaged sea level pressure is applied to study the interannual variability of climate, and the results from CGCM and AGCM are compared to identify the effects of air-sea interaction.

II. MODEL

Both the AGCM and CGCM are developed in Institute of Atmospheric Physics (IAP): The CGCM is a coarse resolution gridpoint model in a uniform terrain-following coordinate. The two components (AGCM and OGCM) have the same horizontal resolution of 4 degrees in latitude and 5 degrees in longitude, but two vertical layers for the AGCM (Zeng et al., 1987; Zeng et al., 1989) and four layers for the OGCM (Zhang and Liang, 1989; Zhang et al, 1992). The AGCM has reproduced satisfactorily many aspects of the contemporary climate (Zeng et al., 1990a; Xue, 1992). The OGCM is successful in simulating major lagre-scale features of the world ocean general circulation,especially for the upper oceans (Zeng et al., 1990b; Zhang et al., 1992). At the air-sea interface, a method similar to flux-correction is applied, i.e. only the anomalous fluxes relative to uncoupled model climates are exchanged each other in order to diminish the initial climate drift resulted from inconsistency of surface fluxes of the uncoupled AGCM and OGCM. The time step for coupling is one month, which is favorable in filtering out synoptic perturbation in the coupling process, but may involve some remarkable asynchronization of at least one component model with its 'boundary' condition provided by another component model. To solve this problem, the so called 'prediction-correction' technique is used for the time integration of the coupled model. At first, the OGCM is integrated over one month to reach an intermediate state; then with the new sea surface condition, the AGCM is run also over one month to get a new state, and finally re-integrate the OGCM over one month to get a new state (Zhang et al., 1992).

III. ANALYTIC METHOD

a. *Rotated EOF Method*

The quantity of data employed here is very large, therefore the rotated Empirical Orthogonal Function (EOF) method is applied to extract the principal temporal and spatial characteristics from the original data. The rotated EOF method is developed on the basis of general EOF method (Horel, 1981), which has the following advantages: the eigenvector produced by the rotated EOF is more reliable and reasonable than that by the general one, and the eigenvector field is similar to the teleconnection pattern obtained from one point correlation map.

b. *Classification of Interannual Variability*

The seasonal mean data are used in our analyses. In such series, the most significant period is the annual cycle. Besides the annual cycle, there is an interannual scale fluctuation which may be obtained usually using the annual mean or typical monthly anomaly (e.g. January or July). In doing so some signals of interannual vraiabilty could be lost. The interannual fluctuation may be divided into two types of variations, as shown in Fig.1 which is an idealized schematic diagram. Two idealized temporal series are shown in Fig.1a and Fig.1b respectively, each series shows two different frequencies, one is *w1*, another is *w2*. Where w1 is the interannual variation and *w2* is the annual cycle. Here *w1* is much smaller than *w2*. In Fig.1a *w1* and *w2* are superimposed according to Eq.(1) below. In Fig.1b *w1* and *w2* are superimposed according to Eq.(2) below. In Fig.1a, the annual amplitude is constant, but the annual mean has an interannual variation, which is defined as the first type of interannual variability of climate and is abbreviated as IVC1 in this paper; in Fig.1b, the annual mean hardly varies with time, but the annual amplitude has interannual variation, which is defined as the second type of interannaul variability of climate and is abbreviated as IVC2 in this paper. These two types of interannual variability can be describled by the following equations:

$$\text{Linear formula:} \quad X(t) = \sin(w2 \times t) + \sin(w1 \times t) \ , \tag{1}$$

$$\text{Nonlinearformula:} \quad X(t) = (A + \sin(w1 \times t)) \times \sin(w2 \times t) \ . \tag{2}$$

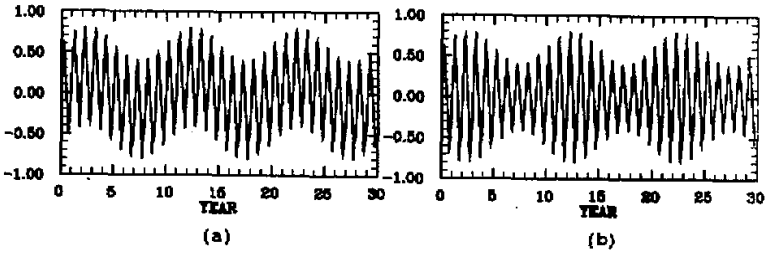

Fig.1. Idealized curve of IVC1 (a) and IVC2 (b) with time.

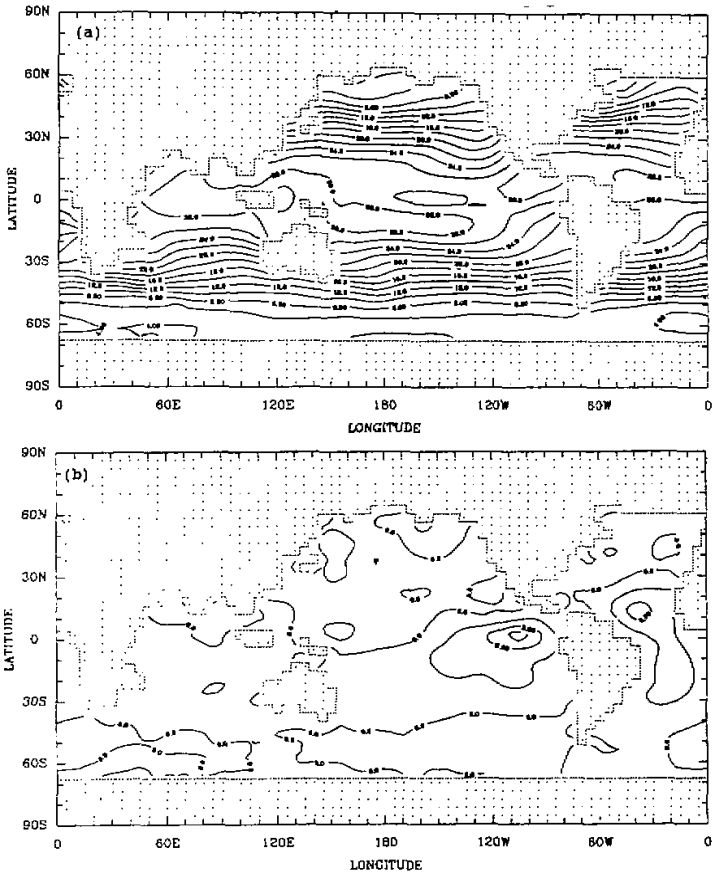

Fig.2. Annual mean SST simulated by IAP CGCM (a) and annual difference, IAP CGCM minus IAP OGCM (b).

Now the interannual variability has been divided into two types——IVC1 and ——IVC2, which represent the interannual variation of the annual mean and amplitude, respectively. In this paper, IVC1 can be obtained by filtering the seasonal anomaly of the sea level pressure with low pass, and the IVC2 is the difference between the sea level pressures for summer and winter.

IV. SIMULATION OF THE MEAN CLIMATE STATE

Xue (1991) pointed out that IAP AGCM simulated successfully the mean climate state. By analyzing the results by IAP CGCM, no great difference can be found between simulations of the mean climate state by IAP CGCM and AGCM (The figures have not been

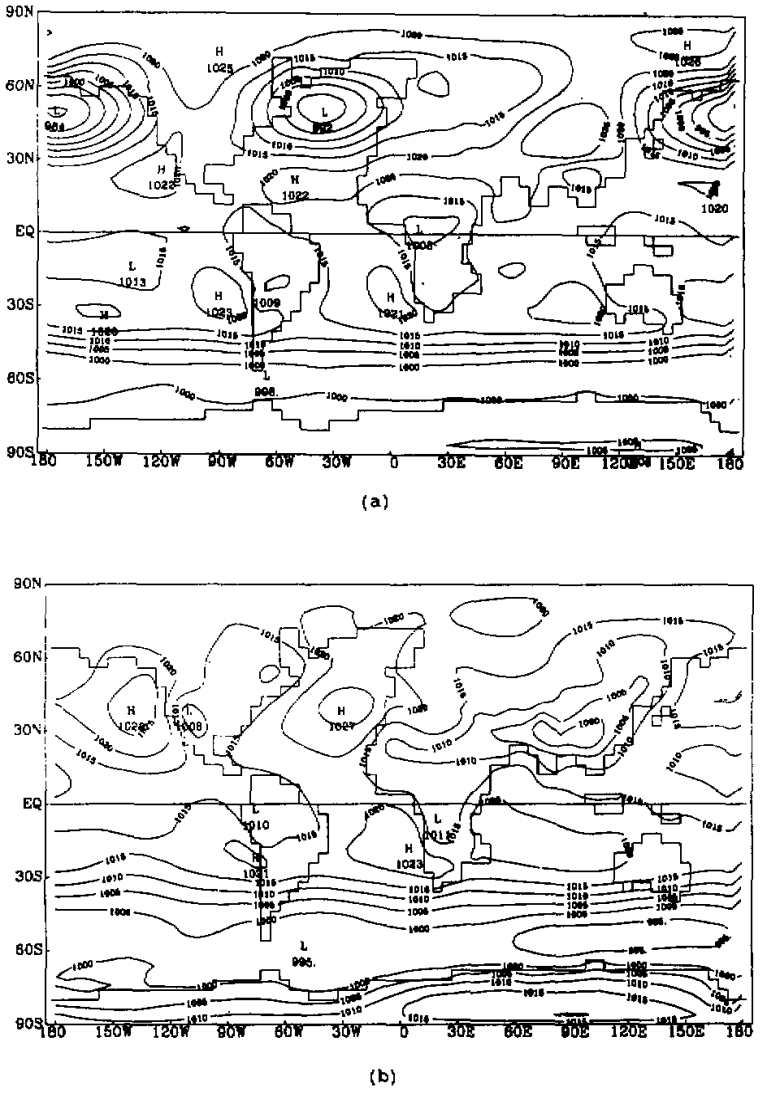

Fig.3. Monthly mean sea level pressure field for January (a) and February (b).

given here), which means that no serious 'climate drift' exists in the IAP CGCM simulation. The simulations of the sea surface temperature (SST) and sea level pressure are given as follows.

a. *Sea Surface Temperature*

Fig.2a shows the global distribution of the annual mean climatological SST simulated by

IAP CGCM. It can be found that the warm pool and cold tongue are correctly simulated. The difference of the annual mean between the CGCM simulation and the uncoupled OGCM simulation is shown in Fig.2b. The major difference with a maximum of about 2 degrees occurs in the eastern tropical Pacific and northern tropical Atlantic. Roughly speaking, the simulated SST is in a good agreement with the observed one. In addition, although the method similar to flux–correction is applied to the coupling scheme, the ENSO–alike phenomenon can be found in the CGCM simulation (Chen, 1992).

b. *Sea Level Pressure*

IAP CGCM may reproduce almost all the atmospheric active centers and principal large scale patterns for January and July (see Fig.3), but their positions and intensities have certain errors. For example, although the high pressure center over high latitude continent and low pressure over high latitude ocean are simulated in January, the highs are weaker and the lows are stronger than observations. Moreover, the South Asia monsoon low located east to observations in July.

V. STANDARD DEVIATION AND TELECONNECTION PATTERN

a. *Standard Deviation*

At each gridpoint, the standard deviations of the monthly mean sea level pressure simulated by AGCM and CGCM in two representative months (January and July) are calculated according to following equation:

$$\sigma = \sqrt{\frac{\sum_{i=0}^{N}(x_i - \bar{x})^2}{(N-1)}} \tag{3}$$

Where, x_i is the sea level pressure of the typical month, $\bar{x}$ is the mean value of the sea level pressure of typical month for several years, N is the sample size, σ represents the standard deviation which reflects the magnitude of the interannual variation. In order to study the the effect of the ocean–atmosphere interaction on the interannual variation, the zonally averaged ratio of the standard deviations of the monthly sea level pressure simulated by CGCM to that by AGCM is shown in Fig.4. In this figure, the four curves represent four months—January, April, July and October. In the middle and high latitudes, the ratio is about 1.0, but in the low latitudes, the ratio is much greater than 1.0, which means that the ocean–atmosphere interaction mainly increases the standard deviation in the tropical region. Xue (1991) has analyzed the standard deviation in the simulation by IAP AGCM, he suggested that the standard deviation in the simulation by AGCM is only half of that for observations in the tropical region. Therefore it can be believed that the CGCM can simulate the real standard deviation better. Charney (1981) has also obtained the similar results. This figure also shows that there is a maximum of ratio in July and minimum of ratio in January in the tropical region.

The geographical distributions of the ratio in January and July are shown in Fig.5a and 5b. Similar to Fig.4, the greatest ratio can be found in the tropical region,

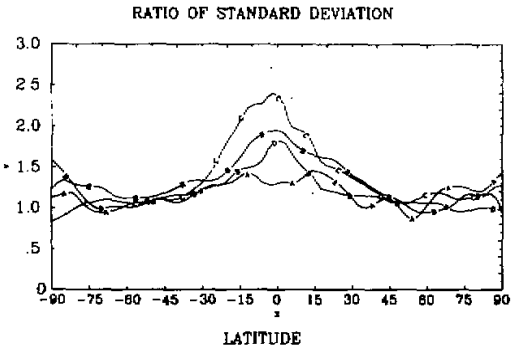

Fig.4. Zonally averaged ratio of the standard deviation simulated by IAP CGCM to that by IAP AGCM for January (curve A), April (curve B), July (curve C) and October (curve D).

especially over tropical Pacific, and the ratio in July is much greater than that in January over the tropical region, which may mean that the ocean–atmosphere interaction has a great effect on the interannual variation in the northern summer especially in the tropical east–middle Pacific. This phenomenon may be related to the so called El Nino.

b. *Teleconnection Pattern*

Sometimes, for example, during the El Nino phase, flood, drought and serious cold may occur simultaneously in various regions over the globe. From a viewpoint of the atmospheric circulation, when an atmospheric active center enhances or decreases, another one may have the same or negative change, which results in anomalous climate occurring simultaneously over the globe. This is so called teleconnection. Walker (1932) found the interannual see–saw of the sea level pressure between Indonesia and the eastern Pacific and defined it as Southern Oscillation (SO) and first put forward the concept of teleconnection. Wallace (1981) analyzed the sea level pressure and 500 hPa potential height field and found several famous teleconnection patterns: North Atlantic Oscillation (NAO). North Pacific Oscillation (NPO) and Pacific North America pattern etc. In this section, the one point correlation map method used by Wallace (1981) is introduced to analyze the teleconnection patterns of the monthly mean sea level pressure in January. The observed Southern Oscillation from Trenberth and Shea (1987) is shown in Fig.6b which is the one point correlation map of the sea level pressure with the base point near Darwin. There are a significant positive correlation region (greater than 0.4) around Australia and Indonesia and a significant negative correlation region (less than −0.4) around the eastern Pacific in Fig.6b. The negative correlation region has two centers in tropical and northern midlatitude region, respectively. On the same one point correlation map (not shown here) as Fig.6b except for that simulated by the AGCM (Xue, 1991), only the significant positive correlation region can be found. There is no significant negative region. It means that the AGCM cannot simulate the Southern Oscillation. Fig.6a shows the

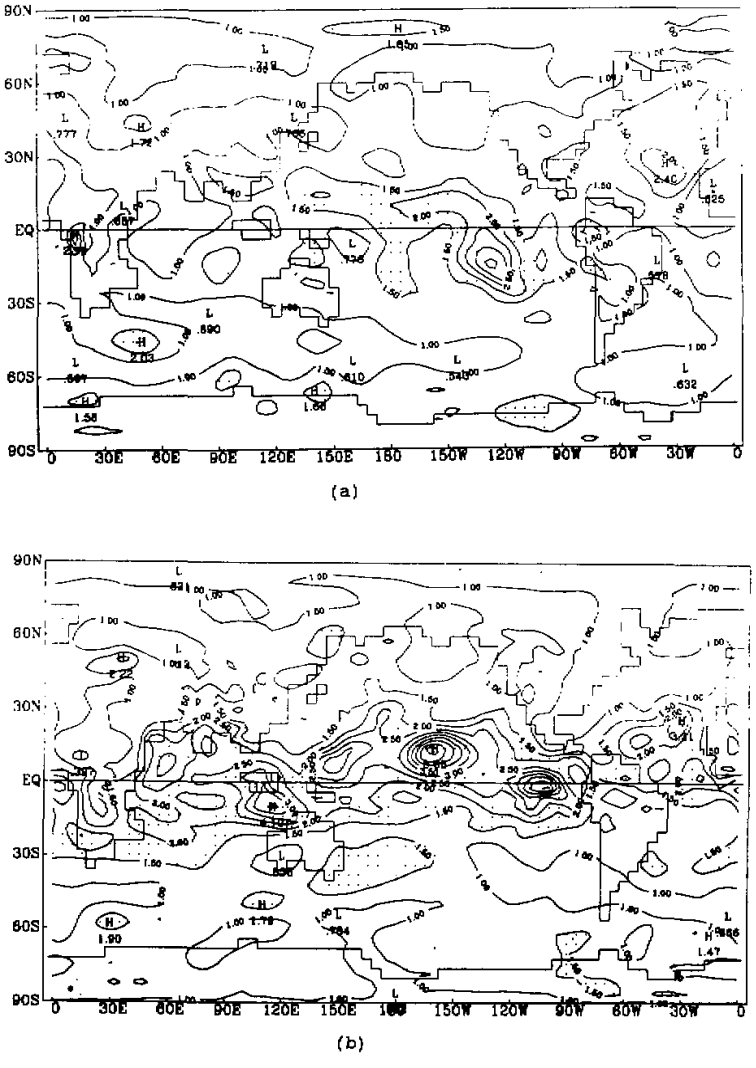

Fig.5. Global distribution of the ratio of the standard deviation as in Fig.4 for January (a) and July (b). Dotted regions indicate that the ratio is greater than 1.5.

same one point correlation map as Fig.6b except for that from the CGCM simulation, the significant positive and negative correlation region located over the western and eastern Pacific Ocean, respectively, and the two centers of significant negative correlation region have the same location as the observed ones. However the significant difference is that the simulated positive correlation region reaches the east of dateline, which may be resulted from the fact

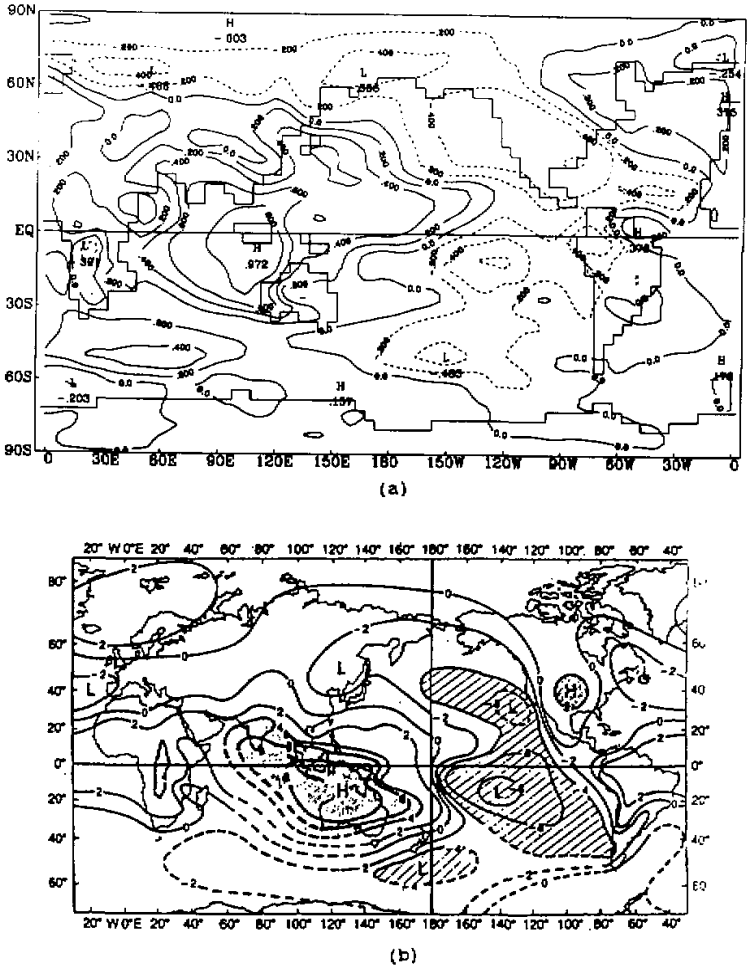

Fig.6. One point correlation map based on the point (6°S / 120°E) or IAP CGCM (a) and observation (b).

that the greatest difference between SSTs from CGCM and observation occurs in the tropical central Pacific (Fig.2b).

The CGCM can simulate not only the Southern Oscillation, but also the North Atlantic Oscillation (see Fig.7). This figure is also a one point correlation map, the base point (66°N–20°W) is near the Iceland Low, the negative correlation center is around 30°N–20°W. This pattern is similar to the observed North Atlantic Oscillation. Xue (1991) analyzed the teleconnection patterns of the sea level pressure simulated by AGCM, and found the AGCM doesn't simulate SO and NAO instead of PNA pattern and teleconnection pattern in the Southern Hemisphere. According to the analyses above, the CGCM can simulate NAO and

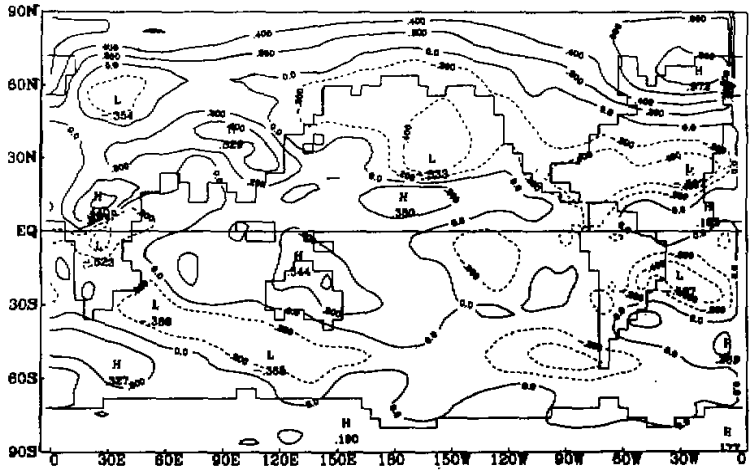

Fig.7. Same as Fig.6 except for 66°N–20°W.

SO patterns, and also the other two teleconnection patterns (not shown here). Therefore some teleconnection patterns may be simulated by both AGCM and CGCM, but others (for example, NAO and SO) can only be simulated by CGCM, which may mean that the ocean–atmosphere interaction can produce NAO and SO patterns.

VI. FEATURES OF TWO TYPES OF INTERANNUAL VARIABILITY

According to the analytic approach in section 3, the two types of interannaul variability of climate (IVC1 and IVC2) are extracted from the AGCM and CGCM simulations. By means of variance and rotated EOF method, the features of IVC1 and IVC2 are studied as follows.

a. *Variance Analyses*

In order to analyze the variance contribution of IVC1 and IVC2, the seasonal anomaly of the sea level pressure is used to caculate power spectra. There are two maximums in the period of three years and about one year, respectively. The former repesents the variance contribution of IVC1, whereas the latter represents the variance contribution of IVC2 because the superimposed period of IVC2 and the annual cycle is about one year. Therefore the variance percentage contributions of IVC1 and IVC2 can be derived from power spectra analyses.

The zonally averaged variance percentage contribution of IVC1 and IVC2 from AGCM and CGCM are calculated and shown in Fig.8a and 8b, respectively. Curve A and B represent variance percentage contribution for AGCM and CGCM, respectively. In these two figures, the variance contribution of IVC1 and IVC2 for AGCM hardly varies with latitudes.

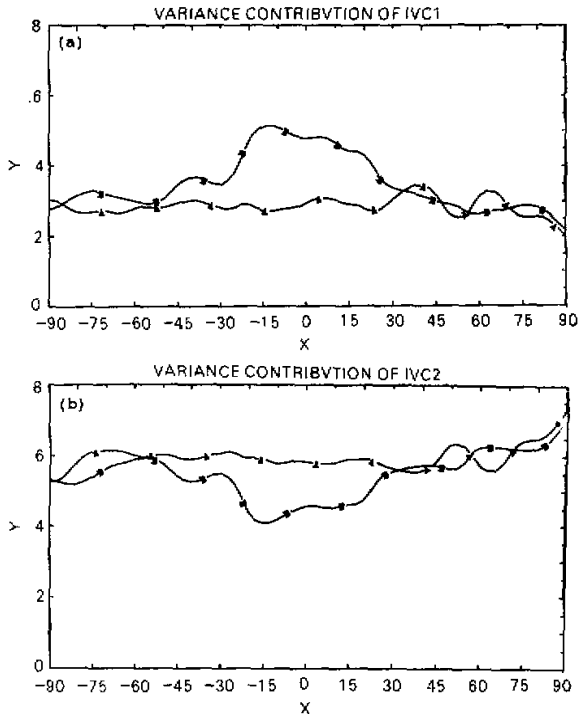

Fig.8. Zonally averaged variance percentage contribution for IVC1 (a) and IVC2 (b). Curve A is from IAP AGCM and B from IAP CGCM.

However those for CGCM have evident maximum or minimum. Fig.8a and 8b also show that the variance contribution of IVC1 and IVC2 for AGCM is almost equal to those for CGCM in the middle and high latitudes, but different in the tropical region. For example, the variance contribution of IVC1 for CGCM is much greater than that for AGCM in the tropical region. The variance contribution of IVC2 for CGCM is less than that for AGCM in the tropical region. In addition, the variance contribution of IVC2 for AGCM and CGCM is much greater than IVC1 in the middle and high latitudes. Theses results suggest that the IVC2 explains the most part of the total variance in the middle and high latitudes and the ocean–atmosphere interaction mainly increases the first type of interannual variability (IVC1) in low latitudes.

b. *The Characteristics of IVC1*

In this section the rotated EOF method is used to analyze the characteristics of IVC1. The first eigenvectors calculated from IVC1 simulated by CGCM and AGCM are shown in Fig.9a and 9b and explain 23.5% and 22.5% of the total variance, respectively. Fig.9a shows that the principal characteristics of IVC1 from CGCM is the Southern Oscillation. The signif-

icant positive and negative correlation region can be found over the western and eastern Pacific. There are three negative correlation centres—one in tropical region and others in middle latitudes. This pattern is the same as the observed Southern Oscillation (Fig.6a). Fig.9b shows the principal characteristics of IVC1 from AGCM, the Southern Oscillation can not be found in this figure. Because the ocean–atmosphere interaction mainly increases the first type of interannual variability (IVC1), the major pattern of IVC1 for CGCM shows the Southern Oscillation. It means the Southern Oscillation can be only generated through the coupled ocean–atmosphere system. The result is the same as that from one point correlation map in Section 5.

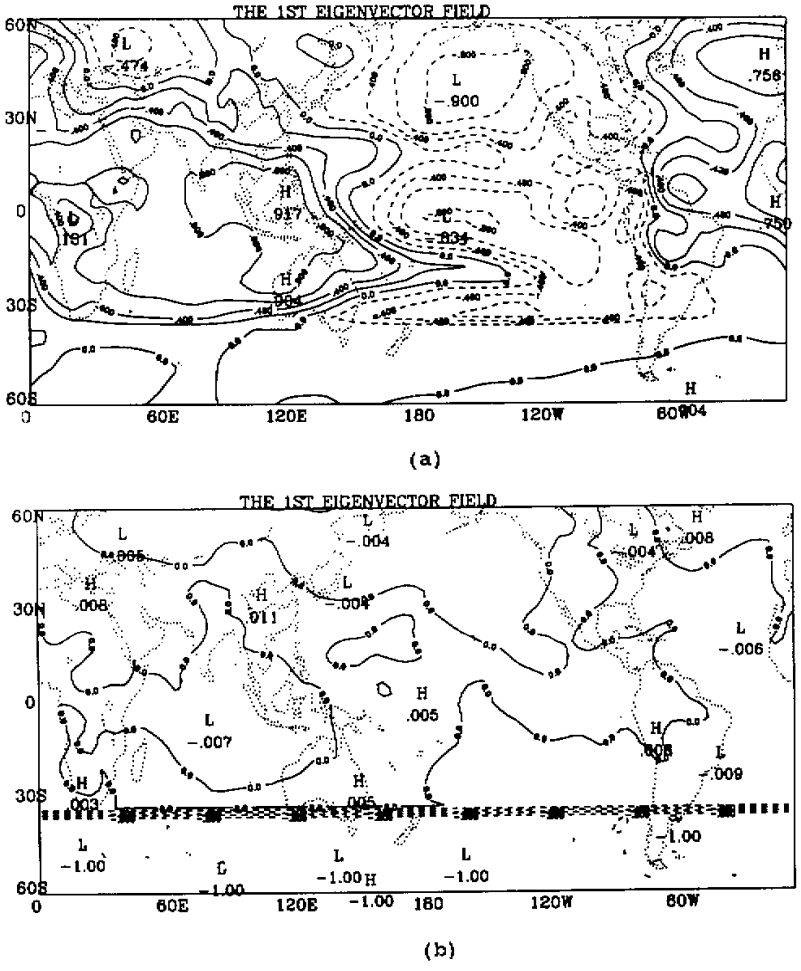

Fig.9. The first eigenvector fields calculated from IVC1 for IAP CGCM (a) and AGCM (b).

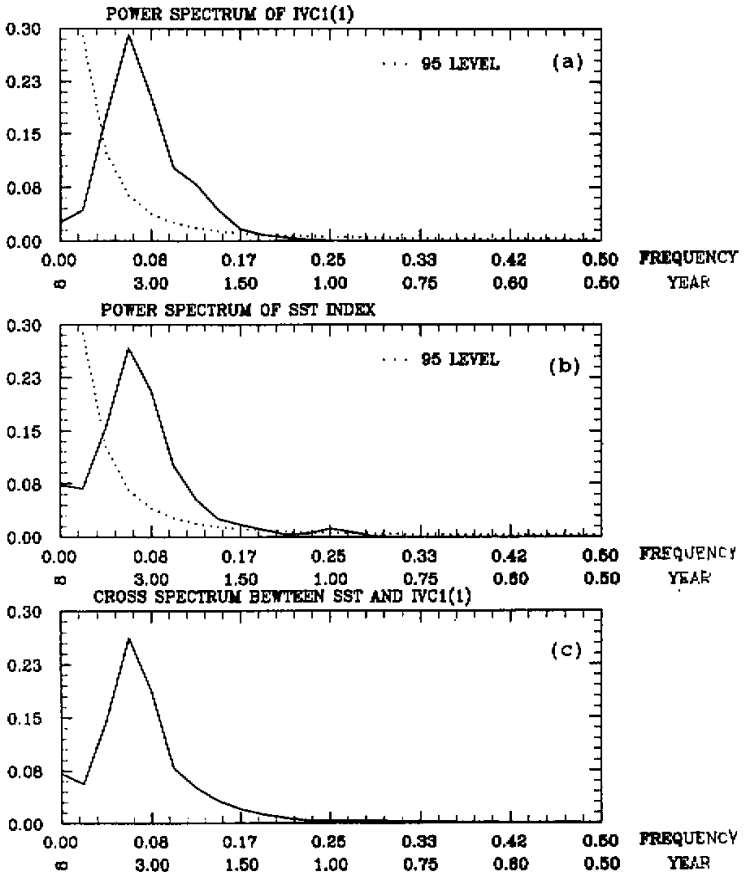

Fig.10. (a) Power spetrum of the first component of IVC1 for IAP CGCM (solid line) and the corresponding red noise curve (dashed line). (b) Power spetrum of SST index for IAP CGCM (solid line) and corresponding red noise curve (dashed line). (c) Cross spectrum between SST index and the first componet of IVC1 for IAP CGCM.

The power spectra of the first principal component of IVC1 for CGCM are shown in Fig.10a, the dashed line represent red noise curve whose significant level is 95%. The most significant period is about 4 years in Fig.10a. In addition, the SST index is obtained through filtering the regional averaged seasonal anomaly of SST over the eastern Pacific with low pass. Fig.10b shows the power spectra of the SST index, the major period is also four years. The observed data have shown that the tropical SST can affect strongly the Southern Oscillation. Therefore the cross spectral analyses between SST index and the first principal component of IVC1 for CGCM are used to find their relation. The cross spectrum (Fig.10c)

indicate that the major period is about 4 years and the coagulation coefficient is about 0.9, which means that there is a very close relation between the SST index and Southern Oscillation.

c. *The Characteristics of IVC2*

Here the IVC2 simulated by AGCM and CGCM are analyzed by means of rotated EOF method in various regions, this is because more details can be found in this way. The first eigenvectors calculated from IVC2 simulated by AGCM and CGCM for the Pacific are shown in Fig.11a–b. Although the principal patterns for CGCM and AGCM are different, the same characteristics are also found in these figures. All patterns show some kinds of meridional stationary wave distributions. Some patterns reflect the meridional distribution in

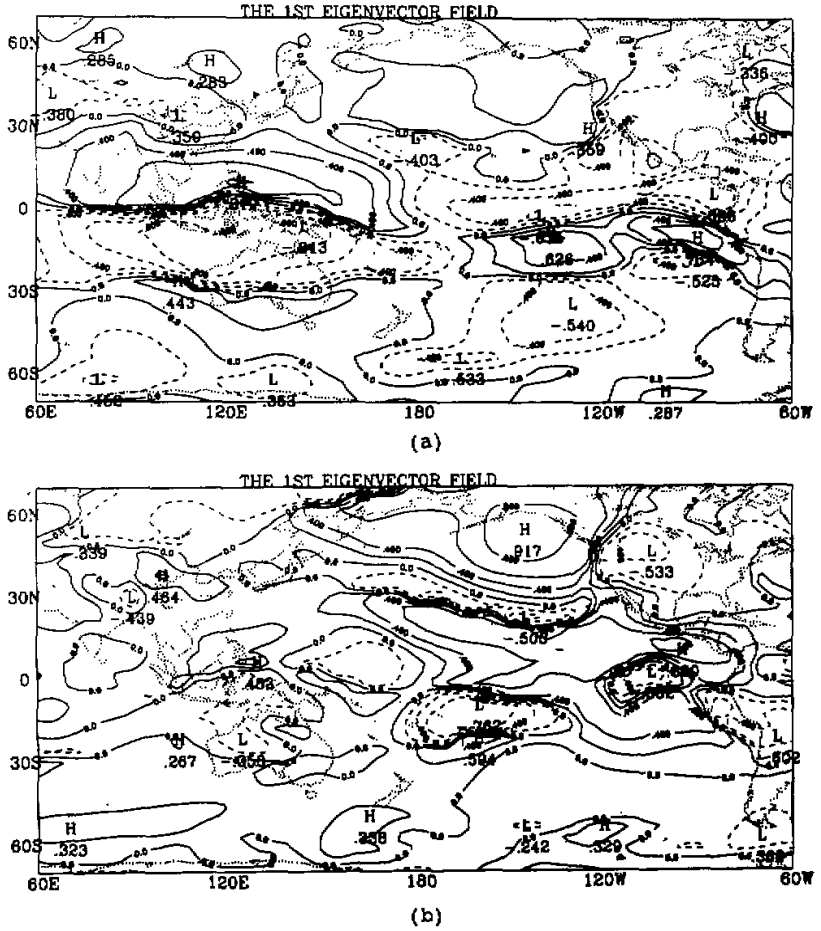

Fig.11. Same as Fig.9 except for IVC2.

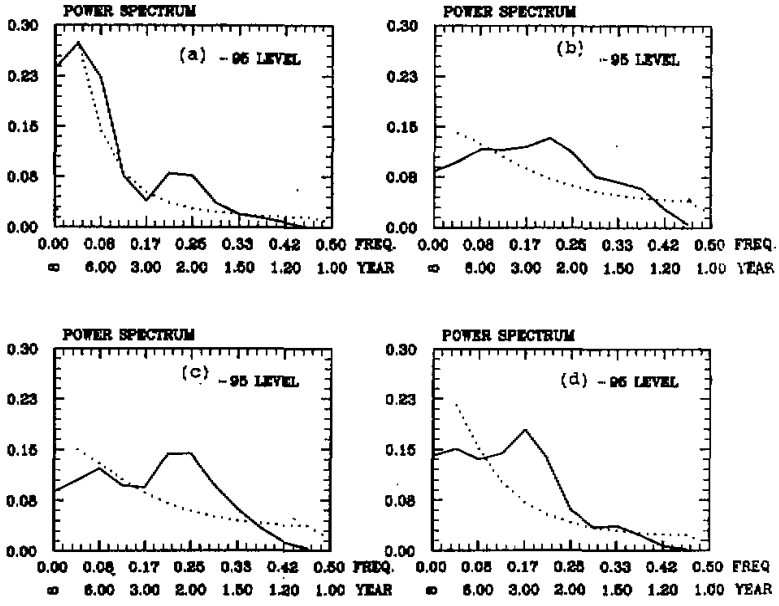

Fig12. Power spectrum of the first (a,c) and second (b,d) principal components of IVC2 for AGCM (a,b) and CGCM (c,d).

the tropical region. Others reflect the meridional distribution in the middle and high latitudes. In addition, the first eigenvector of IVC2 for CGCM over the North Atlantic Ocean is similar to the observed North Atlantic Oscillation, but that for AGCM is not.

The power spectra of the first principal component calculated from IVC2 by CGCM in the four regions above are shown in Fig.12a–d. The dashed lines are the red noise curve of 95% significant level. It can be found that the major period is about 2 years and is less than that from IVC1. IVC2 might have relation with quasi–binnial ocsillation, but further study should be carried out in order to verify it.

VII. CONCLUSION AND DISCUSSION

In this paper, the 25–year integration simulated by IAP AGCM and 40–year integration simulated by IAP CGCM are analyzed, the principal conclusions are as follows:

The CGCM can reasonably simulate the mean climatic state as the AGCM because of the use of a specially designed coupling scheme which controls efficiently the 'climate drift' over the 40–year integration.

By comparing the 40–year integration of the CGCM with the 25–year integration of AGCM, we have found that the ocean–atmosphere interaction can affect the interannaul climatic variability and teleconnection patterns. The standard deviation of the monthly mean sea level pressure obtained from the CGCM is much greater than that from the AGCM in the tropical region, which means that the ocean–atmosphere interaction mainly increases the annual mean variation in the tropical region. In addition, the CGCM can simulate the Southern Oscillation and North Atlantic Oscillation, but the AGCM cannot.

The interannual variability may be classified into two types. One represents the

interannual variation of the annual mean, another represents the interannaul variation of the annual amplitude. We found that the ocean–atmosphere interaction mainly increases the first type of variability. In addition, the principal characteristics of the first type of variability from the CGCM is just the Southern Oscillation, but those from the AGCM don't show this pattern. The principal characteristics of the second type of variability both from the CGCM and the AGCM are possibly some kind of meridional stationary wave patterns.

REFERENCES

Charney, J.G., and J. Shukla (1981), Predictability of monsoons, Monsoon Dynamics, edited by Lighthill and Perace, 99–199.

Chen, K.M., X.H. Zhang, Q.C. Zeng (1992), The features of interannual variability in a coupled general circulation model, Paper presented at International Workshop of Climate Variability, Beijing, 13–17 July, 1992.

Guo, Y.F., D.D. Houghton (1991), Interannual variability of precipitation in an extended 100–year simulation from a coupled ocean–atmosphere climate model, submitted for the Fifth Conference on Climate Variation, Donver, Colorado, October 14–18, 1991.

Horel, J.D. (1981), A rotated principal component analysis of the Northern Hemisphere 500 mb height field. *Mon. Mea. Rev.*, **109**: 2080–2082.

Manabe, S. (1983), Oceanic influence on climate–studies with mathematical models of the Joint–atmosphere system. Large–scale Oceanographical Experiments. WCRP Publ. series, No.1,WMO, p.544.

Meehl, G.A. (1990), Seasonal cycle forcing of El Nino–Southern Oscillation in a global coupled ocean–atmosphere GCM, *J. Climate*, **3**: 72–98.

Neelin J.D., M. Latif, M.A.F. Allaart, M.A. Cane,U. Cubasch, W.L. Gates, P.R. Gent, M. Ghil, C.Gordon, N.C. Lau, C.R. Mechoso, G.A., Meehl, J.M. Oberhuber, S.G.H. Philander, P.S. Schopf, K.R. Sperber, A. Sterl, T. Tokika, J. Tribbia, and S.E. Zebiak (1992), Tropical air–sea interaction in general circulation models, *Climate Dynamics*, **7**: 73–104.

Trenberth, K.E. and D.J. Shea (1987), On the evolution of the Southern Oscillation, *Mon. Wea. Rev.*, **115**: 3078–3096.

Walker, G.T. and E.B. Bliss (1932), World Weather, V. Memoirs, A. Meteor. Soc., **4**: No.36, 53–64.

Wallace, J.M., D.S. Gutzler (1981), Teleconnection in the geopotential height field during the Northern Hemisphere, *Mon. Wea. Rev*, **109**: 785–812.

WMO / ICSU (1984), Scientific plan for world climate research programme WCRP publication series, No.2, WMO / TD–NO. 6, p.95.

Xue, F. (1991), The diagnoses analyses and validation of climate simulation of IAP AGCM, Doctoral Thesis of IAP / CAS (in Chinese).

Zeng, Q.C., C.G. Yuan, X.H. Zhang, X.Z. Liang, N. Bao (1987), A global gridpoint general circulation model. In the collection of Papers Presented at the WMO / IUGG NWP Symposium, Tokyo, 4–8 Aug, 1986, Special Volume of *J. Met. Soc.* Japan, 121–142.

Zeng, Q.C., X.H. Zhang, X.Z. Liang, C.G. Yuan, and S.F. Chen (1989), Document of IAP Two–Level AGCM. TR044, DOE / ER / 60314, –H1, U.S. DOE., Feb., 1989, p.383.

Zeng, Q.C., C.G. Yuan, X.H. Zhang, X.Z. Liang, N. Bao and W.Q. Wang (1990a), IAP GCM and its application to the climate studies, p. 303–330, The Third International Summer Colloquium on Climate Change, Dynamics and Modelling (edited by Zeng et al.), 390pp.

Zeng. Q.C., X.H. Zhang, C.G. Yuan, R.H. Zhang, N. Bao, and X.Z. Liang (1990b), IAP oceanic general circulation models, p. 331–372, The Third Interantioal Summer Colloquium on Climate Change, Dynamics and Modelling (edited by Zeng et al.), China Meteorological Press, Beijing, 390pp.

Zhang, X.H., X.Z. Liang (1989), A numerical world ocean general circulation model, *Adv. Atmos. Sci*, **6**: 44–61.

Zhang, X.H., N. Bao and W.Q. Wang (1991), Numerical simulation of seasonal cycle of world ocean model, Annual Report of LASG / IAP, 1989, 193–203.

Zhang, X.H., N. Bao, R.C. Yu and W.Q. Wang (1992), Coupling scheme experiments based on an atmospheric and oceanic GCM, Chinese *J. of Atmos. Sci*, **16**: No.2, 129–144.